

ICONE  
Conference Paper

American Society of Mechanical Engineers (ASME) owns all copyright and publication subject to this requirement: "Verbatim reproduction of this paper by anyone will be permitted by ASME provided appropriate credit is given to the author(s) and ASME."

## THORIA-BASED CERMET NUCLEAR FUEL: NEUTRONICS FUEL DESIGN AND FUEL CYCLE ANALYSIS

### Thomas J. Downar

Purdue University  
School of Nuclear Engineering  
West Lafayette, IN, 47907-1290  
(765) 494-5752; [downar@ecn.purdue.edu](mailto:downar@ecn.purdue.edu)

### Sean M. McDeavitt

Argonne National Laboratory  
Chemical Technology Division  
9700 S. Cass Avenue  
Argonne, IL 60439  
(630) 252-4308; [mcdeavitt@cmt.anl.gov](mailto:mcdeavitt@cmt.anl.gov)

### S. T. Revankar, A. A. Solomon

Purdue University  
School of Nuclear Engineering  
West Lafayette, IN, 47907-1290

### T. K. Kim

Argonne National Laboratory  
Reactor Analysis and Engineering Division  
9700 S. Cass Avenue  
Argonne, IL 60439

### ABSTRACT

Cermet nuclear fuel has been demonstrated to have significant potential to enhance fuel performance because of low internal fuel temperatures and low stored energy. The combination of these benefits with the inherent proliferation resistance, high burnup capability, and favorable neutronic properties of the thorium fuel cycle produces intriguing options for advanced nuclear fuel cycles. This paper describes aspects of a Nuclear Energy Research Initiative (NERI) project with two primary goals: (1) Evaluate the feasibility of implementing the thorium fuel cycle in existing or advanced reactors using a zirconium-matrix cermet fuel, and (2) Develop enabling technologies required for the economic application of this new fuel form.

This paper will first describes the fuel thermal performance model developed for the analysis of dispersion metal matrix fuels. The model is then applied to the design and analysis of thorium/uranium/zirconium metal-matrix fuel pins for light-water reactors using neutronic simulation methods.

### INTRODUCTION

This paper is one of three in this proceedings describing a 1999 NERI project designed to develop the potential and demonstrate the feasibility of a (Th,U)O<sub>2</sub> cermet fuel [1,2]. The

fundamental nuclear and thermal modeling is described here and the basic fuel concept and experimental cermet fabrication method[1] and the developmental fuel microsphere fabrication method[2] will be described in the other papers.

The principal goal of this project is to demonstrate the feasibility of a metal-matrix dispersion, or cermet, fuel comprising (Th,U)O<sub>2</sub> microspheres in a zirconium matrix that can achieve high burnup and subsequently be directly disposed as nuclear waste. The potential benefits that may be gained with this fuel include high actinide burnup, inherent proliferation resistance, improved irradiation stability due to low internal fuel temperatures, low fuel failure rate, and minimal waste treatment. The cermet fuel concept is shown schematically in Fig. 1. The fuel "meat" is a fine dispersion of (Th,U)O<sub>2</sub> microspheres that have a theoretical density between 70 and 99 % and a uranium enrichment of U-235 below 20%. Nominal values for the microsphere diameter, ThO<sub>2</sub>-to-UO<sub>2</sub> ratio, fuel-to-matrix ratio, and U-235 enrichment were selected as ~50 μm, 50:50, 50:50, and ~19.5 %, respectively, to provide guidance for the calculational and experimental activities carried out within the project [3].

### OVERVIEW OF BASIC COMPUTATIONS

In order to compare the fuel cost and proliferation resistance properties of the proposed dispersion fuel with a

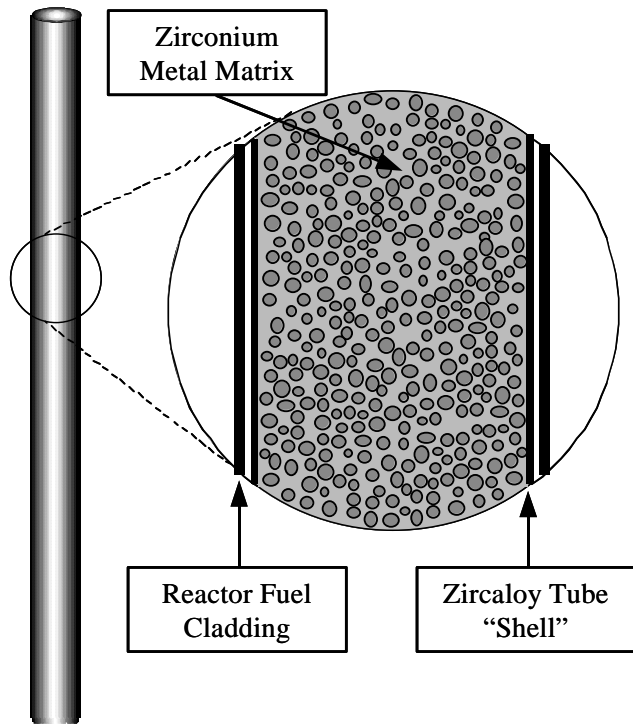


Figure 1. Concept Sketch for (Th,U)O<sub>2</sub> Dispersion Fuel Pin.

typical PWR fuel, fuel pins with different compositions and geometries were analyzed using the Studsvik/Scandpower HELIOS neutronics code and the CORRA economics codes under the same operation conditions. The CORRA fuel cost and proliferation resistance assessment code was developed at Purdue University. The analysis was then extended to full core analysis of a typical PWR loaded with dispersion fuel and standard PWR fuel. The U.S. NRC codes PARCS and RELAP5 were used for the analysis.

Fuel compositions and geometric properties for the pin designs were chosen in order to provide a consistent comparison between dispersion and typical PWR fuel pins. A typical PWR fuel and two different types of dispersion fuels were examined. Both dispersion fuels have a 40 volume percent zirconium matrix and a 60 volume percent heavy metal oxide dispersion, but then respective heavy metal compositions are 9.75% enriched (Th+U)O<sub>2</sub> and 19.5% enriched UO<sub>2</sub>. The highly enriched UO<sub>2</sub> dispersion fuel has been used in this feasibility study to examine a one-batch, 10-year operation core concept.

In order to increase the conversion ratio of the dispersion fuel, the moderator-to-fuel volume ratio of the dispersion pin cell is reduced compared to the typical PWR pin cell. In addition, homogeneous and micro-heterogeneous fuel pin designs were used for the (Th+U)O<sub>2</sub> dispersion composition. Representative fuel cost data and proliferation resistance data were used in the CORRA code.

The results showed that the cycle length of dispersion fuel (661 EFPD) is about two times longer than the PWR (323 EFPD) because of the longer critical burnup of dispersion fuel. The very high cycle length of the highly enriched dispersion fuel (2661 EFPD) demonstrates the possibility for one-batch, 10-year operation with dispersion fuel. The required heavy metal mass of dispersion fuel is smaller than that of the PWR for the fixed cycle length and thermal power, and the dispersion fuel can generate much more thermal power than PWR for the given heavy metal and fixed cycle length. With the baseline assumptions used in the analysis, the fuel cost of dispersion fuel is about 38% higher (e.g., from 3.560 to 4.901 mill/kWh) or use "mills per kilowatt lower" 93% higher (from 3.560 to 6.871 mill/kWh) than the typical PWR. This is mainly due to the separate work utilization of high-enriched dispersion fuel. However, the dispersion fuel has superior proliferation resistant properties because the discharged dispersion fuel is contaminated by U-232 and has a larger spontaneous fission rate and specific decay heat than discharged PWR fuel.

### THERMAL PERFORMANCE MODEL

The accurate thermal modeling of the fuel is an important aspect of reactor safety analysis. The knowledge of the fuel temperature profile is needed not only for the thermal-hydraulics design of the core but also for the neutronic calculations and materials stress analysis. The performance of the fuel rod is related to the safety of the reactor and hence the thermal modeling is an important part of the new composite fuel design. The thermal modeling of composite fuels requires a somewhat different approach than that used for conventional oxide fuels used in most light water reactors.

The thermal modeling of the composite fuel differs from the standard uranium oxide fuel or mixed oxide fuel (uranium and thorium oxide) in two ways. First, the thermal conductivity of the composite material has to be evaluated. The data on the thermal conductivity for composite is limited and, for the composite nuclear fuel, there is no public data. Second, the nature of the composite itself complicates the thermal calculation. The composite adds several variables to the design; hence, the calculations have to be performed for varying conditions to arrive to an optimum design condition.

In the following section, a general methodology is first introduced for predicting the effective thermal conductivity of arbitrary particulate composites with interfacial thermal resistance in terms of an effective medium approach combined with the essential concept of Kapitza thermal contact resistance [4]. Using this method, the composite fuel thermal conductivity is calculated. The uranium and thorium oxide mixed fuel is taken as the composite particle and the metal matrix structure is taken as the base medium. Various combinations of the particulate size and fractions are used for the calculation. The heat transfer from the composite fuel rod to the coolant is solved as a steady-state heat transfer problem. The fuel pin clad, temperature, pin average temperature and the radial pin temperature, profile are obtained.

## Effective Conductivity Model For Metal Matrix Composites

The thermal properties of metal-matrix composite materials have received substantial attention in recent years because of their potential use as packaging materials in electronic applications. The thermal boundary resistance that exists between the particle and base matrix interface largely affects the thermal conductivity of the composite. Interfacial thermal contact resistance between different constituent phases in a composite can arise from the combination of poor mechanical/chemical adherence at the interface and thermal expansion mismatch. For small particles, the thermal boundary resistance can, in effect, turn ceramic particles into non-conducting entities and reduce the effective conductivity to well below that of the matrix. This phenomenon is related to the fundamental processes of heat transfer at the interface.

For an ideal interface, the thermal resistance is known as the Kapitza resistance, after the discovery by Kapitza in 1941 [5] of the temperature discontinuity at the interface between liquid He and Cu due to heat flow. Recent models of the phonons (heat treated as a particle, similar to a photon) scattering at the ideal interface explain, in part, the temperature discontinuity observed. The effective medium theory is based on the multiple scattering processes at the interface. For a given heat flux through the metal-ceramic interface, a temperature difference,  $\Delta T$ , develops across the interface; it is related to the heat flux as follows:

$$Q = \frac{\Delta T}{R_{BD}},$$

where  $R_{BD}$  is the thermal boundary resistance. The shape of the particle has a strong effect on  $R_{BD}$ . The thermal conductivity of the composite,  $K_{eff}$ , depends on  $R_{BD}$  for spherical mono dispersed particles as follows:

$$K_{eff} = K_m \frac{[K_p (1 + 2\alpha) + 2K_m] + 2f[K_p (1 - \alpha) - K_m]}{[K_p (1 + 2\alpha) + 2K_m] - f[K_p (1 - \alpha) - K_m]}$$

where  $K_p$  and  $K_m$  are the thermal conductivities of the metal and the ceramic particle, respectively,  $f$  is the volume fraction of the particles, and  $\alpha$  is a dimensionless parameter. It is defined as

$$\alpha = \frac{R_{BD} K_m}{a}$$

Here,  $a$  is a particle radius. The parameter  $\alpha$  is a measure of the influence of the particle boundary resistance on the thermal conductivity of the particle. When  $\alpha$  is large,  $R_{BD}$  dominates, and when is small,  $R_{BD}$  is negligible. By defining a Kapitza radius as  $a_k \alpha \equiv R_{BD} K_m$ ,  $a_k$  is related in a simple model to the mean free path of phonons divided by the probability of phonon transmission at the interface. Typical values of Kapitza resistance,  $R_{BD}$ , are in the range of  $10^{-9}$  to  $10^{-8}$  ( $m^2K/W$ ) for SiC

and Al composites. In order to see the effect of the particle size on the effective thermal conductivity, an example is shown in Fig. 2 for  $UO_2$  as spherical particles in Zircaloy metal matrix with particle volume fractions  $f$  of 50% and 75%. The properties used for the calculations are given in Table 1.

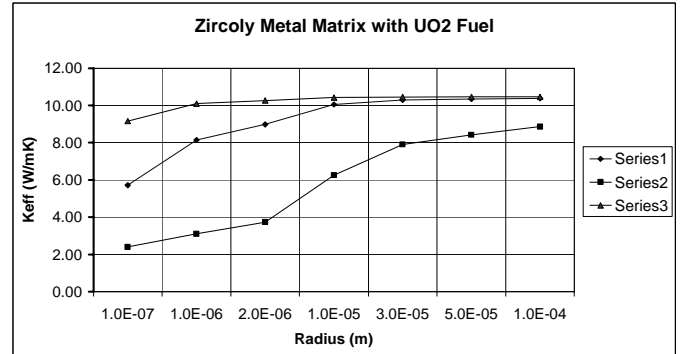


Figure 2. Effective Thermal Conductivity of  $UO_2$  Ceramic-Zircaloy Metal Matrix Composite. (Series 1.  $f = 50\%$ ,  $T = 500K$ ., Series 2.  $f = 75\%$ ,  $T=500K$ , Series 3.  $f = 50\%$ ,  $T = 1500K$ ).

Table 1 Thermal Conductivities for Particle and Metal Matrix

Material	Temperature (K)	K (W/mK)
Zr-Alloy	500	12.7
$UO_2$	500	8.4
Zr-Alloy	1500	21.6
$UO_2$	1500	2.6

From Fig. 2, it is seen that whenever  $a \gg a_k$  ( $\alpha$  is small), the particle is large enough that thermal boundary resistance is negligible. Conversely, when  $a \ll a_k$  ( $\alpha$  is large), thermal boundary resistance dominates. The transition region from one regime to the other occurs around  $a \approx a_k$  ( $\alpha \approx 1$ ).

### One-Dimensional Heat Transfer Model

Consider the cross section of the composite fuel rod geometry as shown in Fig. 3.  $R_F$ ,  $R_{Cl}$  and  $R_{CO}$  are the fuel pellet radius (m), clad inside radius (w/m-k), and clad outside radius (m) respectively. The steady-state heat conduction equation for the fuel rod is given as

$$\frac{1}{r} \frac{d}{dr} \left( kr \frac{dT}{dr} \right) + q''' = 0$$

where  $T$  is the temperature ( $^{\circ}C$ ),  $q'''$  is the heat flux ( $W/m^3$ ), and  $k$  is the thermal conductivity ( $W/m$ ).

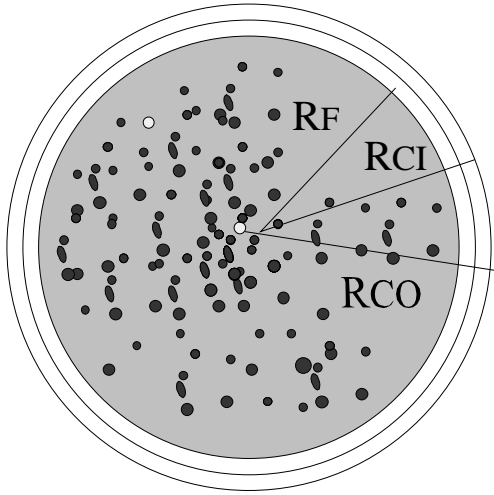


Figure 3. Cross-Sectional View of the Composite Fuel Rod.

**Fuel Region** For the fuel region, integrating the heat conduction equation twice and using these boundary conditions:

$$r = 0: q''' / r = 0 = -k \frac{dT}{dr} /_{r=0} = 0,$$

and

$$r = R_F: T = T_{FO},$$

the solution is

$$\int_{T_{FO}}^{T_{\max}} k dT = \frac{q'}{4\pi}$$

where the linear heat rate is  $q' = \pi R_{FO}^2 q'''$ . The radial temperature profile is calculated from

$$\int_T^{T_{FO}} k(T) dT = -\frac{q'''}{4} (R_{CO}^2 - r^2).$$

If the thermal conductivity  $k$  in the fuel is assumed as constant, then the fuel average temperature,  $T_{AVE}$ , is given as,

$$T_{AVE} - T_{FO} = \frac{1}{2} (T_{\max} - T_{FO}) = q' / 8\pi k$$

**Gap conductance model** The heat transfer at the gas gap is given in terms of the heat flux:

$$q'''_{gap} = h_g (T_{FO} - T_{CI})$$

where  $h_g$  is the gas gap heat transfer coefficient. For fresh fuel (open gap) as

$$h_g = \frac{k_{gas}}{\delta_{eff}} + \frac{\sigma}{\frac{1}{\epsilon_F} + \frac{1}{\epsilon_C} - 1} \frac{T_{FO}^4 - T_{CI}^4}{T_{FO} - T_{CI}}$$

Here,  $k_{gas}$  is the thermal conductivity of the gas,  $\delta_{eff}$  is the effective gap width,  $\sigma$  is the Stefan-Boltzman constant  $(5.669 \times 10^{-8} \text{ W/m}^2\text{K}^4)$ , and  $\epsilon_F$  and  $\epsilon_C$  are surface emissivities of the fuel and cladding respectively. The effective gap width is calculated as follows:

$$\delta_{eff} = \delta_g + \delta_{jump1} + \delta_{jump2}$$

where  $\delta_{jump1}$ , and  $\delta_{jump2}$  are correction gaps due to temperature discontinuity at the gas-solid surface. A typical value at atmospheric pressure for the sum of  $\delta_{jump1} + \delta_{jump2}$  is  $10\mu\text{m}$  (helium) and  $1\mu\text{m}$  (xenon). A typical gap conductance for a PWR fuel rod at 14 kW/ft (460 W/cm) is 1000 BTU/hr-ft<sup>2</sup> F or  $0.575 \text{ W/cm}^2 \cdot ^\circ\text{C}$  (fresh fuel).

**Heat Transfer Between the Coolant and Rod** The heat transfer between the coolant and the rod is expressed in terms of the Nusselt number,  $Nu$ , and the heat transfer coefficient,  $h$ , for rod bundles.

$$Nu = \left( \frac{h D_e}{k_c} \right) = C Re^{0.8} Pr^{1/3}$$

Where  $D_e$  is the effective hydraulic diameter. The Reynolds number,  $Re$ , and Prandlt number,  $Pr$ , are given as follows:

$$Re = \frac{\rho U D}{\mu}$$

and

$$Pr = \frac{\nu}{\alpha}$$

Here the  $U$  is the liquid velocity and  $D$  is the channel hydraulic diameter and  $\mu$  is the viscosity and  $\nu$  is the kinematic viscosity,

$$\left( \frac{\mu}{\rho} \right)$$

The constant,  $C$ , depends on the pitch-to-diameter ratio,  $P/D$ , and is given as  $C = 0.026 (P/D) - 0.006$  for a triangular array, and  $(1.1 \leq P/D \leq 1.5)$  and  $C = 0.042 (P/D) - 0.024$  for a square array  $(1.1 \leq P/D \leq 1.3)$ .

**Overall Rod Thermal Resistance** The rod overall temperature drop is calculated in terms of the series thermal resistances across the fuel pin, gap, cladding, and clad outside surface. The

temperature drop between the rod centerline and the rod outer surface is given as

$$T_{\max} - T_{CO} = q' \left[ \frac{1}{4\pi\bar{k}_f} + \frac{1}{2\pi R_g h_g} + \frac{1}{2\pi k c} \ln \left( \frac{R_{CO}}{R_{CI}} \right) \right]$$

Here,  $\bar{k}_f$  is the constant thermal conductivity of pallet (composite fuel). This is obtained from the effective conductivity model described in the previous section.  $R_g$  is the mean gap radius.

### Thermal Performance Model Results

A Fortran program was developed to calculate the effective thermal conductivity and temperature profile in the composite fuel rod based on the effective conductivity model for the composite fuel and the heat transfer model described in the previous sections. Table 2 gives the list of input parameters used in the calculation and sample output of the calculation. Calculations were performed to examine the following parameters: (1) fuel and metal matrix composition (% from 30-70 to 70-30), (2)  $UO_2$  and  $ThO_2$  composition (% from 30-70 to 70-30), (3) fuel particle size (from 1  $\mu m$  to 100  $\mu m$ ), and (4) fuel theoretical density (% from 90 to 100).

Table 2. Sample Calculation Results

Input Parameters	
Core Inlet Temperature	$t_{in} = 569.11$ K
Core Outer Temperature	$t_{out} = 601.00$ K
Water Mass Flux	$g_l = 3500.240$ kg/m <sup>2</sup> ·s
Rod Linear Heat Rate	$q_{lin} = 17519.00$ W/m
Subchannel Triangle-1, Square-0	$st = 0$
Fuel Rod Diameter	$d = 0.0097$ m
Rod Pitch	$p = 0.0128$ m
Clad Thickness	$cl_{dtk} = 0.6350E-03$ m
Gap Thickness	$\delta = 0.00E+00$ m
Composite % of (Th,U)O <sub>2</sub>	$disp = 50.00$ %
Fuel particle size	$a = 0.100000E-03$ m
Volume Fraction of Fuel	$f = 0.5000$
Kapitza Resistance (m <sup>2</sup> K/W)	$r_{bd} = 0.100E-07$
Volume % of Metal Matrix	$tdzr = 0.100000E+03$
Volume % of Oxide Fuel	$tdox = 0.100000E+03$
Calculated Results	
Liquid Bulk Temperature	= 585.05 K
Clad Outer Wall Temperature	= 598.18 K
Clad Inner Wall Temperature	= 621.75 K
Fuel Outer Surface Temperature	= 621.75 K
Fuel Average bulk Temperature	= 693.22 K

In Fig. 4, the effect of the Kapitza resistance on the temperature profile of the composite fuel rod is shown. For large Kapitza resistances, the fuel rod temperature is higher. The temperature profiles for different volume fractions of the oxide fuel in the metal matrix are shown in Fig. 5. Higher fuel volume fraction gives higher temperature levels in the fuel rod. In Fig. 6, the fuel rod temperature profiles are shown for different fractions of  $ThO_2$  in  $UO_2/ThO_2$  fuel-metal matrix composite. The temperature profile is not affected by the fraction of  $ThO_2$  in the  $UO_2/ThO_2$  fuel.

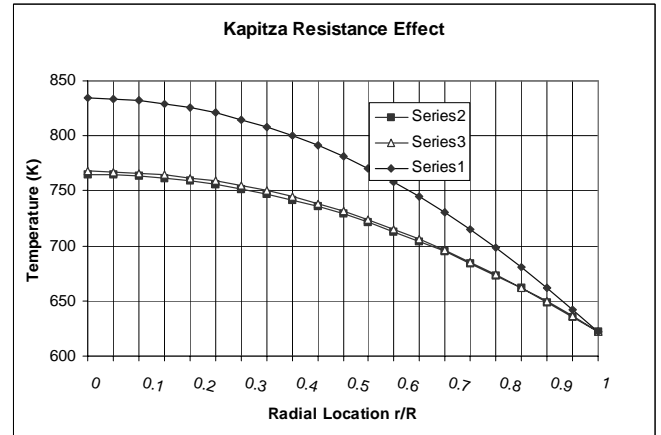


Figure 4. Effect of the Kapitza resistance on the Temperature Profile, (Series 1:  $10^{-4}$  m<sup>2</sup>K/W; Series 2:  $10^{-8}$  m<sup>2</sup>K/W; Series 3:  $10^{-6}$  m<sup>2</sup>K/W);

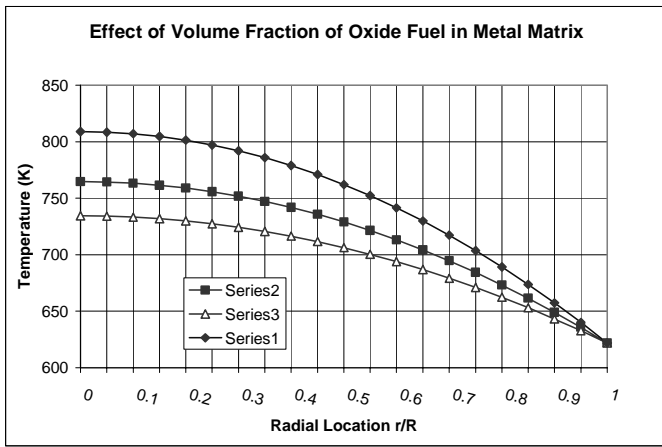


Figure 5. The Temperature Profile in a Fuel Rod for Different Volume Fractions of Fuel (series 1: 50%, series 2: 30%, and series 3: 70% of fuel in metal matrix).

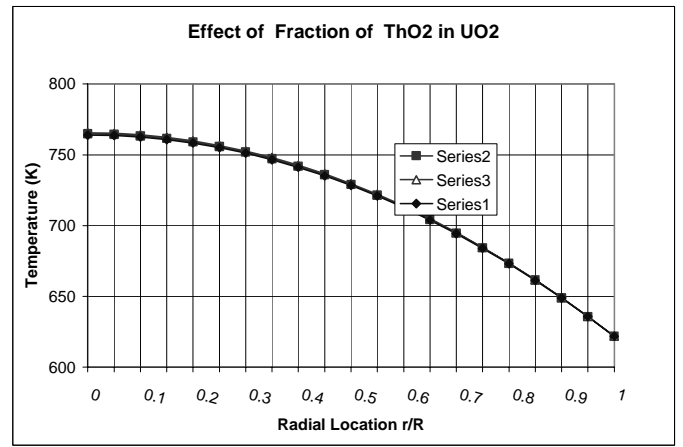


Figure 6. The Temperature Profile for Different ThO<sub>2</sub> fraction in UO<sub>2</sub>-ThO<sub>2</sub> mixed fuel, (series 1: 50%, series 2: 30%, and series 3: 70% ThO<sub>2</sub> in UO<sub>2</sub>-ThO<sub>2</sub> mixed fuel).

Table 3. Summary of Metal Matrix Fuel Pin Sensitivity Study

Factor	Initial $k_{\infty}$	Depletion Rate	Spectrum	Critical Burnup	Remarks
Reference Fuel, (UO <sub>2</sub> 4% enriched)	1.33124	-829 pcm	soft	35.5 MWD/kg	
Zirconium Matrix Volume	decreases	slightly slow	softer	reduced	<ul style="list-style-type: none"> <li>• Reduced heavy isotope</li> <li>• Increased conductivity</li> </ul>
Thorium-to-Uranium Ratio	decreases	slightly slow	-	reduced	<ul style="list-style-type: none"> <li>• Big absorption at BOC</li> <li>• Breeding U233</li> </ul>
Moderator-to-Fuel Ratio	decreases	slow	fast	reduced	<ul style="list-style-type: none"> <li>• Slow depletion due to the fast spectrum</li> <li>• Reduced T/H capability</li> </ul>
Fuel Pin Radius	-	-	-	-	<ul style="list-style-type: none"> <li>• No strong effect</li> </ul>
Fuel Temperature	-	-	-	-	<ul style="list-style-type: none"> <li>• No strong effect</li> </ul>
Moderator Void Fraction	decreases	slow	fast	-	
Pin Power Density	-	-	-	residence time decreases	<ul style="list-style-type: none"> <li>• Residence Time = Burnup/Power Density</li> </ul>

## Metal Matrix Fuel Neutronics Analysis

The thermal performance model was then used in the neutronics analysis of various metal fuel designs. The neutronics calculations were performed using the HELIOS [6] lattice physics code. HELIOS is a multigroup two-dimensional collision probability method transport code for fuel or fuel assembly depletion analysis of thermal reactors. Because the neutron spectrum in the thorium/uranium/zirconium fuel pin cell can be different from a thermal reactor spectrum, the HELIOS code was benchmarked using Monte Carlo depletion analysis codes [7].

### Fuel Pin Design Sensitivity Study

The design of the thorium/uranium/zirconium metal matrix pin was performed by examining several key design parameters which included:

1. Thorium-to-Uranium Ratio
2. Moderator-to-Fuel Ratio
3. Fuel Pin Radius
4. Fuel Temperature
5. Moderator Void Fraction
6. Pin Power Density

The sensitivity of fuel pin neutronics performance on the key design parameters was analyzed using the HELIOS code and the thermal performance model. The results are summarized in Table 3.

The sensitivity studies indicate that the most important factors for increasing the fuel burnup is to increase the initial k-infinite value of the fuel and to reduce the depletion rate (ie. slope of the reactivity versus burnup curve). The three most important design parameters to achieve this are (1) the relative heavy metal/zirconium content of the fuel, (2) the ratio of thorium/uranium, and (3) the moderator to fuel ratio. The impact of each of these on the final pin design is summarized below.

Zirconium Matrix Volume In the sensitivity study on the relative Zr/heavy metal fraction, it was concluded that increasing the amount of Zr softens the neutron spectrum because it displaces the strongly absorbing heavy metal. The initial k-inf values are slightly increased with increasing the Zr volume fractions because of the softer spectrum, however beyond a certain Zr volume fraction the initial k-inf values will decrease with increasing Zr because the total amount of fissile material will be reduced. Therefore, an optimum Zr volume fraction exists and in the sensitivity studies, the optimum value is near 50%. However, because of potential materials considerations with tolerating such a high Zr content, the Zr volume fraction will be set at 40% for future work.

Thorium-to-Uranium Ratio The thorium to uranium ratio in the fuel also requires a tradeoff in considerations since Thorium exhibits contrasting neutronics properties. Thorium behaves like

a poison at BOC because its absorption cross section is larger than U238. However, thorium is a fertile material and the production of U233 is an obvious advantage for extending the fuel burnup. The poison effect reduces the initial k-inf value and the fertility effect increases the cycle length. However, based on the sensitivity studies, the poison effect is dominant and the U233 breeding is not that much more efficient than the breeding of Pu239 by U238. Therefore, in order to increase the initial k-infinite, the Th amount is kept to a minimum. However, because thorium is an important isotope for proliferation resistance, a compromise thorium amount is used which is 50% of the total heavy metal.

Moderator-to-Fuel Ratio A low moderator to fuel volume provides a hard neutron spectrum and reduces the rate of depletion. There are two general approaches to obtain a small Vm/Vf ratio. The first is reduce the fuel pin pitch with a constant fuel radius. The second is to increase the fuel radius with a constant fuel pitch. The former option results in a tight lattice fuel configuration and the latter option is generally referred to as a “fat fuel”. These two methods have very similar nuclear properties. However, the fat fuel has the secondary benefit of increasing the fuel residence time. This can be demonstrated using the following relation between the linear power density ( $q'$ ) and specific power density ( $q'''$ )

$$q' = q''' \times \rho_{HM} \times \pi r_{fuel}^2$$

where

$$\rho_{HM} = \text{density of heavy metal,}$$

$$r_{fuel} = \text{radius of fuel rod.}$$

For a given linear power density, the specific power of a “fat fuel” rod would be lower than that of a typical LWR fuel pin. Because of the enhanced thermal behavior of the Zr-metal fuel, the temperature profile in the metal matrix pin is considerably reduced and it is possible to increase the radius and specific power of the fat fuel without compromising fuel centerline temperature limits. A typical Vm/Vf ratio for a PWR fuel cell is ~ 1.65. In the designs here, a ratio of 1.0 and 1.2 were used for PWR and BWR fuel pins, respectively.

### LWR Fuel Pin Designs

Based on the design parameters for PWR and BWR fuel pins shown in Table 4, pin cell calculations were performed using the HELIOS code and the results are summarized in Tables 5 and 6, respectively. As shown in Table 5, the discharge burnup is greater than 100.0 GWD/t in all PWR cases. The fat fuel pin with 50% thorium and Vm/Vf=1.0 is best because it provides the longest fuel residence time. For the BWR cases, none of the fuel pin design provides a discharge burnup greater than 100.0 GWD/t. However, the residence time of the fat fuel with 50% thorium and Vm/Vf=1.2 is almost double that of the typical BWR fuel pins. The proposal fuel pin designs are shown in Fig. 7, and k-inf behavior of proposed PWR and BWR pins is shown in Fig. 8 and 9, respectively. The

temperature profile across the PWR fuel pin is shown in Fig. 10.

Table 4. Summary of Fuel Pin Design Data

General Data	PWR	BWR
Linear power density (W/cm)	178	206
System Pressure (bar)	155	72
Average void fraction	0	0.4
Fuel pitch (cm)	1.25	1.62
Cladding diameter (cm)	0.94	1.25
Fuel diameter (cm)	0.819	1.056
Average moderator temperature (K)	583	549
Average fuel temperature (K)	900	900

## SUMMARY AND CONCLUSIONS

Metal-matrix cermet nuclear fuels with thorium/uranium compositions have potential for use in a high-burnup, proliferation-resistant fuel cycles. This paper described the neutronics and fuel thermal behavior modeling and analysis performed as part of the Department of Energy NERI project, "Fuel for a Once-Through Cycle-(Th,U)O<sub>2</sub> in a Metal Matrix."

While the work here analyzed metal-matrix cermet fuels within the framework of conventional LWR fuel designs, the full potential of metal-matrix cermet fuels for Generation IV type reactors remains to be examined. Because of the substantially lower fuel temperatures achievable in metal matrix cermet fuels, considerable design flexibility is introduced for advanced reactor concepts. Metal matrix cermet fuels may provide the enabling technology for such attractive concepts as the supercritical temperature/pressure reactor which operates at temperatures well above those currently used in conventional light water reactors.

## REFERENCES

- [1] S.M. McDeavitt, T.J. Downar, S. Revankar, A.A. Solomon, M. C. Hash, and A. S. Hebden "Thoria-Based Cermet Nuclear Fuel: Cermet Fabrication and Behavior Estimates," 10<sup>th</sup> International Conference on Nuclear Engineering, Arlington, VA, April 14-18, 2002, Paper No. ICONE10-22317.
- [2] A.A. Solomon S.M. McDeavitt, V. Chandramouli, S. Anthonysamy, S. Kuchibhotla, and T.J. Downar, "Thoria-Based Cermet Nuclear Fuel: Sintered Microsphere Fabrication by Spray Drying," 10<sup>th</sup> International Conference on Nuclear Engineering, Arlington, VA, April 14-18, 2002, Paper No. ICONE10-22445.
- [3] S.M. McDeavitt, T.J. Downar, M.C. Hash, S. Revankar, A.A. Solomon, Y. Xu, A.S. Hebden, W. Robey, and J. Xiu, "Development of a Mixed-Oxide Cermet Dispersion Fuel Using (Th,U)O<sub>2</sub> in a Zirconium Metal Matrix," *ANS Transactions* 83 (2000) 205.
- [4] Every et al., *Acta. Metall.-Mater.* 40 (1992) 123.
- [5] Kapitza, J. *Phys. (USSR)* 4 (1941) 18.
- [6] F. D. Giust, "Fuel Management System, HELIOS Documentation," Studsvik Scandpower, September 11, 1999.
- [7] X. Zhao, K.D. Weaver, Y. Xu, and T.J. Downar "Comparison of CASMO-4, HELIOS, and MOCUP for ThO<sub>2</sub> Pincell Burnup," *ANS Transactions*, 83 (2000) 197.

Table 5. Summary of PWR Fuel Pin Designs

**PWR Proposal Fuel**

Fuel Tuype	Fuel			Vm/Vf	Power density(W/g)	K-inf				
	Zr (%)	Th/U	Enrichment			BOC	CB*	Slope	DB**	residence***
Typical PWR	0	0/100	3.5	1.65	37.8	1.33939	29.5	-831	44.3	1170.60
Tight	40	50/50	9.75	1.20	63	1.35545	71	-466	106.5	1690.50
Fat	40	50/50	9.75	1.20	53	1.36230	73	-466	109.5	2071.10
	<b>40</b>	<b>50/50</b>	<b>9.75</b>	<b>1.00</b>	<b>48</b>	<b>1.31984</b>	<b>67</b>	<b>-455</b>	<b>100.5</b>	<b>2083.80</b>

\*CB=Critical Burnup

\*\* DB = 3 batch discharge burnup

\*\*\* 3 batch case reference time (day)

Table 6. Summary of BWR Fuel Pin Designs

**BWR Proposal Fuel with 40% void**

Fuel Tuype	Fuel			Vm/Vf	Power density(W/g)	K-inf				
	Zr (%)	Th/U	Enrichment			BOC	CB*	Slope	DB**	residence***
Typical BWR	0	0/100	3.5	1.60	25.9	1.25164	20.5	-674	30.75	1187.26
Tight	40	50/50	9.75	1.20	43	1.25924	55	-431	82.5	1279.07
Fat	<b>40</b>	<b>50/50</b>	<b>9.75</b>	<b>1.20</b>	<b>37</b>	<b>1.26644</b>	<b>57</b>	<b>-432</b>	<b>85.5</b>	<b>2310.81</b>
	40	50/50	9.75	1.00	34	1.22036	47	-407	70.5	2073.53

\*CB=Critical Burnup

\*\* DB = 3 batch discharge burnup

\*\*\* 3 batch case reference time (day)

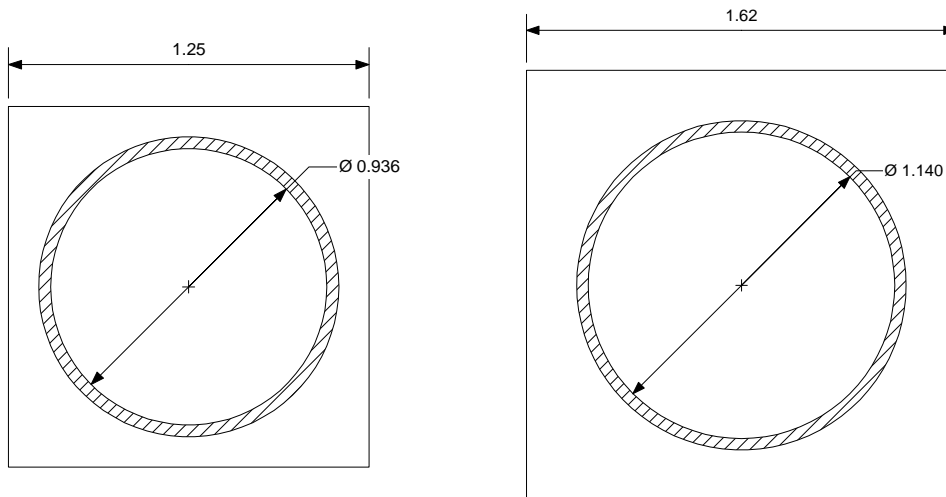


Figure 7. Schematic of Proposed Fuel Pins (left : PWR, right: BWR)

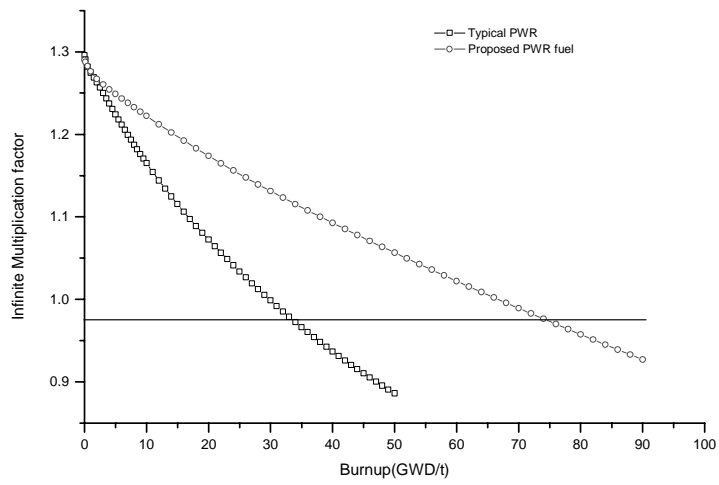


Figure 8. Plot showing the  $k_{\infty}$  versus Burnup Behavior of the Proposed PWR Fuel Pin.

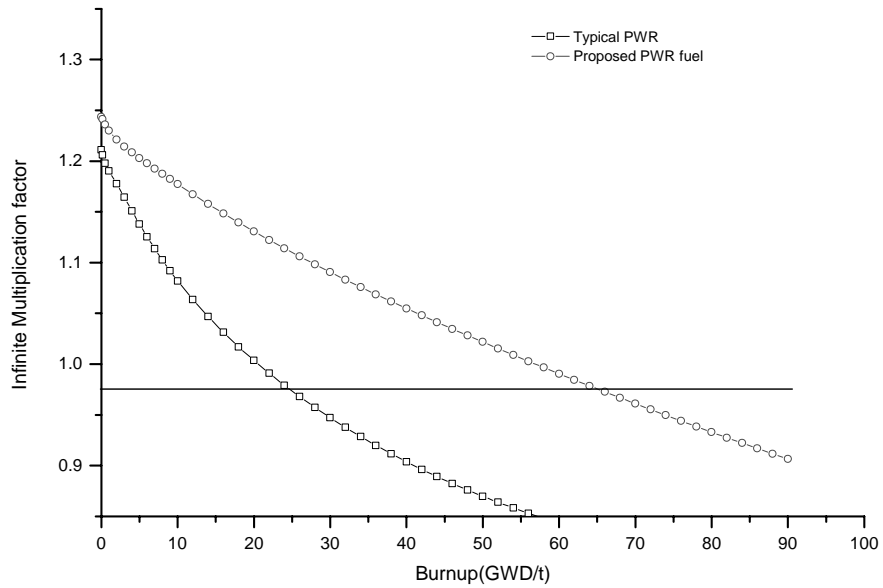


Figure 9. Plot showing the  $k_{\infty}$  vs. Burnup of the Proposed BWR Fuel Pin.

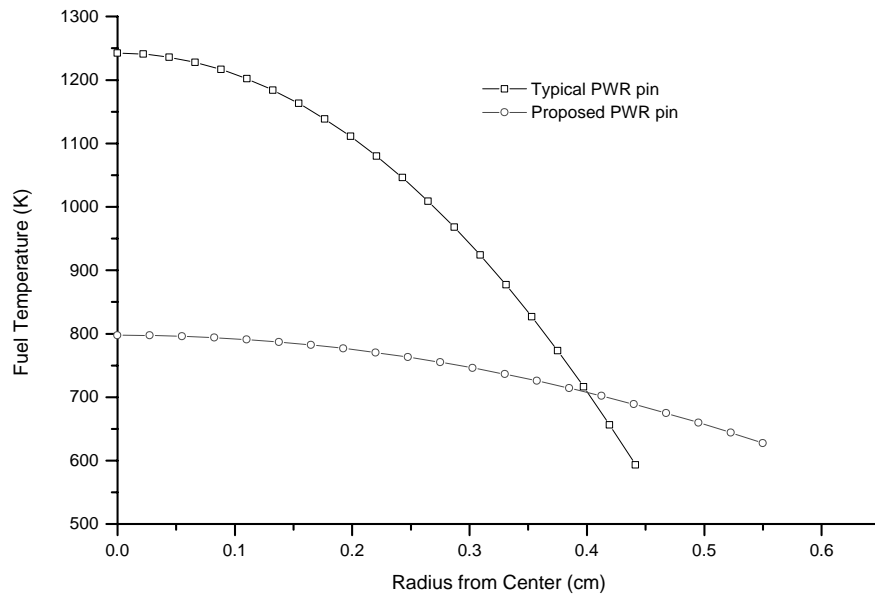


Figure 10. Temperature Profile of the Proposed PWR Fuel Pin .